Microstructure and atomic effects on the electroluminescent efficiency of SrS:Ce thin film devices

W. L. Warren[a] and C. H. Seager
Sandia National Laboratories, Albuquerque, New Mexico 87185-1349

S.-S. Sun
Planar America Incorporated, 1400 North West Compton Drive, Beaverton, Oregon 97006

A. Naman, P. H. Holloway, and K. S. Jones
Department of Materials Science, University of Florida, Gainesville, Florida 32611

E. Soininen
Planar International Limited, P.O. Box 46, SF-02201 Espoo, Finland

(Received 22 April 1997; accepted for publication 14 August 1997)

Transmission electron microscopy and x-ray diffraction data show that rapid thermal anneals of SrS:Ce thin films enhance grain size and reduce crystalline defects. Electron paramagnetic resonance results suggest that these anneals lead to less variance in the crystal field environments at the nearly cubic Ce^{3+} sites along with the formation of another type of Ce^{3+} site believed to involve a nearby Sr vacancy. We suggest that the association of Ce^{3+} sites with V_{Sr} shifts the electroluminescence towards larger wavelengths as the symmetry of the activator site is lowered. [S0021-8979(97)01122-5]

I. INTRODUCTION

Much research and development is being devoted to the improvement and realization of display technologies using both electroluminescent (EL) and electron impact excitation processes.[1–3] Critical properties for display phosphors include chromaticity, brightness, longevity, and efficiency. For materials to exhibit these characteristics, it is necessary to not only incorporate the rare-earth luminescent activators in the host material with the proper oxidation state and crystal field symmetry, but to also control the defect density in the host.

Ce-activated SrS (SrS:Ce) has emerged as one of the promising blue-green emitting phosphor materials for EL devices.[4–10] In this study, we explore the environment of the Ce^{3+} ion (local symmetry, oxidation state, and atomic scale site-to-site fluctuations in the crystal field) in the SrS lattice and directly relate this information to EL performance. We show that it is not necessarily the density of Ce^{3+} centers in the lattice that determines the overall luminescent efficiency for the SrS:Ce film; rather, it appears as though the specific environment at the Ce ion site as well as the elimination of host lattice defects play significant roles in the overall luminescent process.

II. EXPERIMENTAL DETAILS

The SrS:Ce phosphor thin films were prepared by rf magnetron sputtering from targets with $SrS:CeF_3$ (0.12 mol % Ce) both with and without Ga additions. The Ga was incorporated into the target in the form of excess Ga_2S_3; it is believed that the Ga acts as a fluxing agent to promote grain growth.[6] Following the deposition, the films were rapid thermal annealed (RTA) at 650, 750, or 810 °C in a N_2 environment.[6]

For EL characterization, devices were fabricated using an atomic layer epitaxy Al_2O_3–TiO_2 first insulator and a sputter-deposited barium tantalate second insulator. Indium tin oxide (bottom electrode) and Al (top electrode) were deposited so that an alternating voltage could be applied to the device. The electron paramagnetic resonance (EPR) measurements were made using an *X*-band Bruker spectrometer at 14 K. The EPR and EL data were recorded on the same devices so that a direct correlation could be made. The transmission electron microscopy (TEM) and x-ray diffraction (XRD) characterization of the SrS:Ce and SrS:Ce,Ga films were made on samples prepared in a similar way to the ones for the EPR. The EL efficiencies of the samples used in the XRD and TEM studies are within 10% of those samples used for the EPR analysis. Absolute spin concentrations of the Ce^{3+} were determined by comparing the double integrated EPR spectra to that from a calibrated spin standard (strong pitch). The absolute spin densities are accurate to about a factor of 2. The density of the Ce^{3+} sites was determined by computer analysis of the EPR line shapes for the two types of EPR-active Ce^{3+} centers observed.[11,12]

III. RESULTS

A. EL characterization

Figures 1 and 2 show the EL spectral intensity for SrS:Ce and SrS:Ce,Ga EL devices, respectively, annealed at different postdeposition temperatures (as-deposited, 650, 750, and 810 °C. The emission spectra of Figs. 1 and 2 were obtained by operating the EL devices 40 V above their threshold voltages. At temperatures above 750 °C, the films that were codoped with Ga show a marked improvement in EL performance when compared to the non-Ga codoped films.[6] The Ga-doped films also exhibit a greenshift (the emission moves to longer wavelengths) of the emitted color, which becomes more pronounced at higher annealing tem-

[a]Electronic mail: wwarren@sandia.gov

 0021-8979/97/82(10)/5138/6/$10.00

TABLE I. Combined EPR and EL data on SrS:Ce devices that were subjected to differing RTA temperatures.

Sample	Nearly cubic Ce^{3+} density	$Ce^{3+}-V_{Sr}$ density	Total Ce^{3+} density	Linewidth	(CIE coordinates)	EL efficiency
650 °C	$0.8\times10^{19}/cm^3$	$<0.3\times10^{19}/cm^3$	$0.8\times10^{19}/cm^3$ (0.022 at. %)	227 G	(0.202, 0.362)	0.10 lm/W
750 °C	$1.5\times10^{19}/cm^3$	$<0.3\times10^{19}/cm^3$	$1.5\times10^{19}/cm^3$ (0.041 at. %)	188 G	(0.197, 0.358)	0.11 lm/W
810 °C	$1.6\times10^{19}/cm^3$	$\leq0.3\times10^{19}/cm^3$	$1.9\times10^{19}/cm^3$ (0.051 at. %)	110 G	(0.196, 0.361)	0.14 lm/W

peratures. The EL efficiency and CIE coordinates for each of the postdeposition anneal temperatures are given in Tables I and II. The greenshift in the emitted color can also be seen by the increase in the Commission Internationale d'Eclairage (CIE) y coordinate in Table II versus that in Table I.

B. Microstructure

The RTA improved film crystal quality and promoted grain growth for both the Ga and the non-Ga doped films. TEM characterization of the sputter as-deposited SrS:Ce thin films revealed a very fine grained polycrystalline structure with a columnar grain morphology. After annealing at 810 °C, grain growth was observed, however, the grain morphology remained columnar. The as-deposited SrS:Ce,Ga films had grain sizes comparable to the films without Ga additions (Table III). The TEM micrographs in Fig. 3 illustrate that annealing at 810 °C resulted in grain coarsening accompanied by a transformation to a spherullitic grain morphology. These SrS:Ce,Ga films had an average grain size of 600 nm, approximately one-half the total phosphor layer thickness.

C. EPR characterization

In order to obtain microscopic information about the effects of the RTA and for differences between the Ga-doped and non-Ga doped SrS:Ce films, we studied the EL devices using EPR. EPR is sensitive to the crystal field environment of the Ce ion, and can provide quantitative information regarding the concentration of Ce^{3+} ions in the SrS thin film.[10,11,13–15] Figures 4 and 5 show the EPR traces of the same EL devices characterized in Figs. 1 and 2, respectively, while pertinent EPR data are summarized in Tables I and II. The EPR spectra show two types of Ce^{3+} environments. The Ce^{3+} resonance at $g_\perp=1.317$ is found to be orientationally dependent upon rotating the SrS:Ce thin films in the magnetic field; it is characterized by a small axial g-tensor anisotropy ($g_\parallel=1.292$ and $g_\perp=1.317$) as shown in Fig. 6.[15] This particular Ce^{3+} center has been shown to involve a stress-induced displacement of the Ce^{3+} ion along the [111] growth direction of the thin films; this Ce^{3+} center will be termed a nearly cubic Ce^{3+}. An ancillary defect is apparently not the source of the near cubic Ce^{3+} orientational dependence since the degree of anisotropy is dependent on the film growth direction, discussed elsewhere.[15] The linewidth of the nearly cubic Ce^{3+} resonance at $g_\perp=1.317$ can be affected by either Ce^{3+}–Ce^{3+} (magnetic dipole–dipole) interactions,[9,16,17] or atomic-scale fluctuations, i.e., site-to-site variations, in the crystal field around the Ce^{3+} ion. Such fluctuations may be induced by defects, nonuniform film stress, or other structural and/or chemical disorder.

The other Ce^{3+} site ($g_\parallel=0.963$ and $g_\perp=1.525$) exhibits a larger axially symmetric *powder-pattern* line shape. The

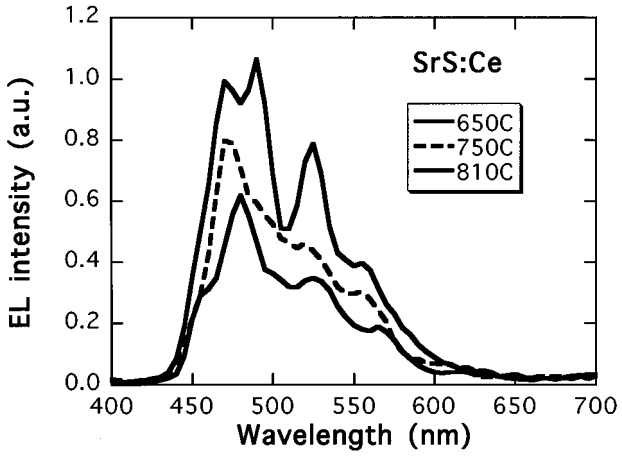

FIG. 1. EL emission spectra of sputtered SrS:Ce films following differing RTA treatments: (a) 650, (b) 750, and (c) 810 °C. The emission spectra were obtained by subjecting the devices to a bias 40 V above their respective threshold voltages.

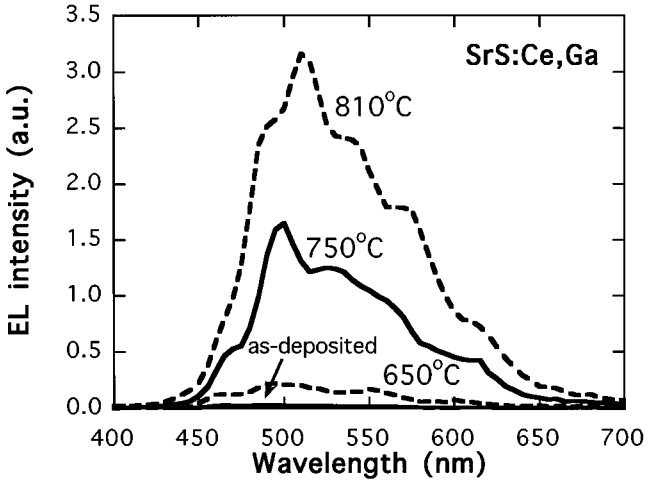

FIG. 2. EL emission spectra of sputtered SrS:Ce,Ga films following differing RTA treatments: (a) as-deposited, (b) 650, (c) 750, and (d) 810 °C. The emission spectra were obtained by subjecting the devices to a bias 40 V above their respective threshold voltages.

TABLE II. Combined EPR and EL data on SrS:Ce,Ga devices that were subjected to differing RTA temperatures.

Sample	Nearly cubic Ce^{3+} density	$Ce^{3+}-V_{Sr}$ density	Total Ce^{3+} density	Linewidth	(CIE coordinates)	EL efficiency
As-deposited	$0.65\times10^{19}/cm^3$	$<0.3\times10^{19}/cm^3$	$0.65\times10^{19}/cm^3$ (0.018 at. %)	450 G	(0.243, 0.390)	0.01 lm/W
650 °C	$1.4\times10^{19}/cm^3$	$0.4\times10^{19}/cm^3$	$1.8\times10^{19}/cm^3$ (0.049 at. %)	173 G	(0.260, 0.445)	0.04 lm/W
750 °C	$1.4\times10^{19}/cm^3$	$0.9\times10^{19}/cm^3$	$2.3\times10^{19}/cm^3$ (0.062 at. %)	121 G	(0.289, 0.509)	0.33 lm/W
810 °C	$1.3\times10^{19}/cm^3$	$1\times10^{19}/cm^3$	$2.3\times10^{19}/cm^3$ (0.062 at. %)	90 G	(0.292, 0.512)	0.61 lm/W

powder-pattern line shape reflects the two principle symmetry directions of the *defect* center (parallel or perpendicular) with respect to the applied magnetic field. The much less intense $g_{\|}$ signal could not be detected in the thin films due to a poor signal to noise ratio; it could only be observed in SrS:Ce powders. However, identical signals at $g_{\perp}=1.525$ were also observed in the powders.[5,11,17] Typically this type of powder-pattern line shape results from an EPR center that exhibits axial symmetry in a completely randomly oriented system, as was found for SrS:Ce powders.[11,12,18] This powder-pattern line shape also exhibits a slight orientational dependence as shown in Fig. 6. The origin of this orientational dependence is the same as that observed for the nearly cubic Ce^{3+} site discussed earlier; these Ce sites are displaced along the [111] film growth direction.[15] Figure 6 shows the *perpendicular* transition of the powder-pattern line shape when the magnetic field is positioned parallel or perpendicular to the growth direction of the SrS:Ce film. We note that in the highly doped SrS:Ce *powders*, this powder-pattern signal does not have an orientational dependence; it only shows a double-peaked axially symmetric line shape.

We suggest that this large axial distortion of this Ce^{3+} site ($g_{\|}=0.963$ and $g_{\perp}=1.525$) is likely caused by the presence of a doubly negatively charged Sr vacancy near the Ce^{3+} ion which allows for charge compensation. A doubly negatively charged Sr vacancy in the lattice perturbs the cubic ligand field around the Ce^{3+} ion; it distorts the Ce^{3+} ''octahedron'' giving rise to the powder-pattern, axially symmetric Ce^{3+} center. As discussed in Ref. 11, the EPR line shape suggests that the Sr vacancy lies in the Sr second nearest neighbor shell in the SrS lattice. This signal is more prevalent in the SrS:Ce,Ga films (Fig. 5), and will be termed the $Ce^{3+}-V_{Sr}$ center. Besides observing this center in SrS:Ce powders and films deposited by rf sputtering, we have also seen this center in SrS:Ce films prepared by atomic layer epitaxy and molecular beam epitaxy. Thus, it appears to be an intrinsic defect center to SrS:Ce.

TABLE III. Combined EPR and EL data on SrS:Ce devices that were subjected to differing RTA temperatures.

Sample	Anneal temperature	FWHM (XRD)	Grain size (nm) from TEM
Ga doped	As-deposited		
	650 °C	0.336	80
	750 °C	0.188	110
	810 °C	0.136	600
Non-Ga doped	As-deposited	0.87	40
	650 °C	0.62	80
	750 °C	0.44	120
	810 °C	0.238	140

1. EPR for the SrS:Ce films (non-Ga doped)

For the postdeposition anneals for the SrS:Ce EL, devices the density of the nominally ''cubic'' Ce^{3+} increases with anneal temperature, but tends to saturate around 750 °C. Data in Table I show that the linewidth of the nearly cubic Ce^{3+} ion resonance decreases appreciably with increasing anneal temperature. The decrease in linewidth may result from the breakup of Ce clustering during RTA, or from the Ce^{3+} crystal field environment becoming more uniform. The

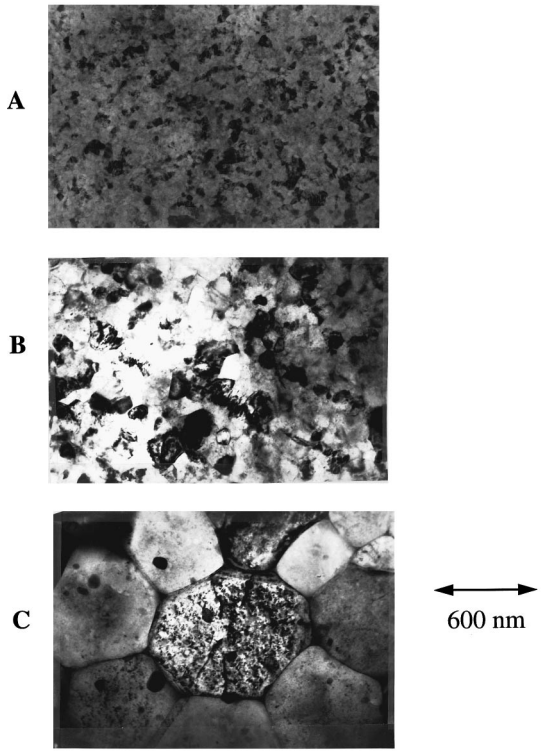

FIG. 3. TEM micrographs of sputtered SrS:Ce,Ga thin films subjected to a (a) 650, (b) 750, or (c) 810 °C RTA.

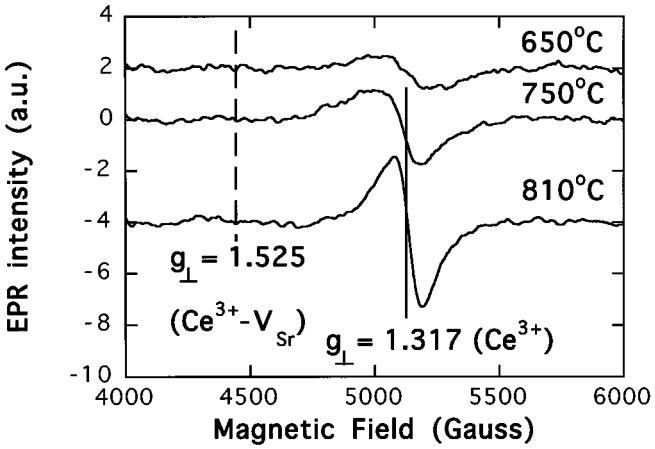

FIG. 4. EPR traces of the same SrS:Ce films used in Fig. 2: (a) 650, (b) 750, and (c) 810 °C.

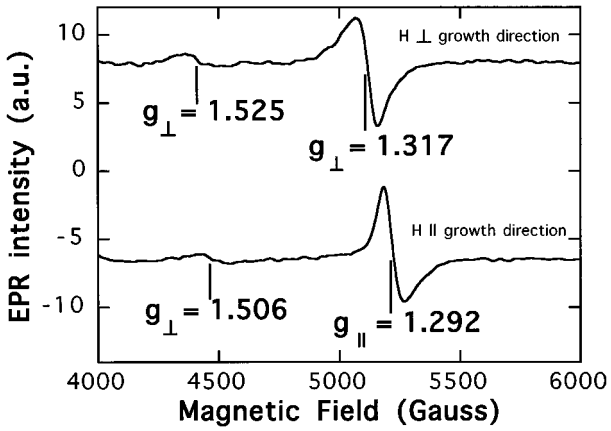

FIG. 6. EPR traces of the SrS:Ce,Ga film given a RTA at 810 °C. The magnetic field is orientated parallel or perpendicular to the film growth direction.

TEM micrographs of these samples (not shown) show grain growth with increasing anneal temperature. XRD analysis shows that the RTA results in a narrowing of the full width at half-maximum (FWHM) of the diffraction peaks, evidence that the anneal improves crystalline quality of the SrS film (Table III). We will conclude that the decreased EPR linewidth of the nearly cubic Ce^{3+} site is better ascribed to a uniform crystal field. The $Ce^{3+}-V_{Sr}$ signal is very weak in intensity in the SrS:Ce devices, thus, it is difficult to establish the strength of this resonance with any degree of accuracy.

2. EPR for the SrS:Ce,Ga films

The density of the nominally cubic Ce^{3+} sites is approximately the same for the Ga codoped EL devices annealed at 650, 750, and 810 °C. Thus, the improved EL performance with anneal temperature cannot be solely attributed to changes in the density of these centers. Table II and Fig. 4 show that the linewidth of the nearly cubic Ce^{3+} ion resonance decreases appreciably with increasing anneal temperature similar to the SrS:Ce devices without Ga codoping. As the anneal temperature increases, the density of centers ascribed to $Ce^{3+}-V_{Sr}$ also increases. Thus, the total Ce^{3+} density increases with anneal temperature for the SrS:Ce,Ga EL devices, but most of it is associated with the $Ce^{3+}-V_{Sr}$ site. This increase in $Ce^{3+}-V_{Sr}$ probably requires higher temperatures because the double negatively charged V_{Sr} vacancies diffuse to the positively charged Ce sites, and form the $Ce^{3+}-V_{Sr}$ complex.[19] The driving force to form these pairs is largely electrostatic.

Note that SrS:Ce,Ga films have larger $Ce^{3+}-V_{Sr}$ signals and larger grain sizes than the non-Ga codoped SrS:Ce films. It has been suggested that Ga codoping can act as a fluxing agent responsible for the enhanced grain growth in the films.[6] The exact mechanism leading to large $Ce^{3+}-V_{Sr}$ densities is unclear, but the Ga flux should increase the rate of diffusion and therefore pair formation.

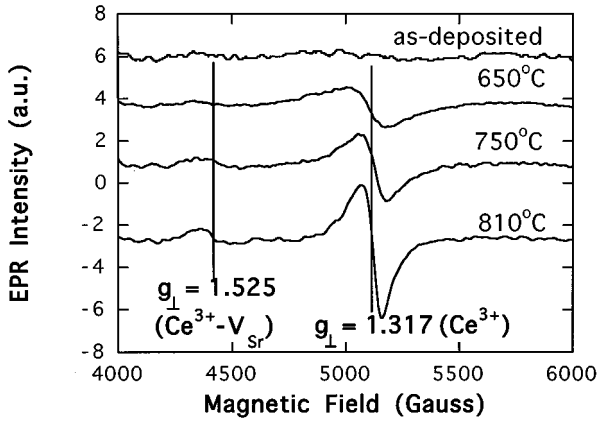

FIG. 5. EPR traces of the same SrS:Ce,Ga films used in Fig. 3: (a) as-deposited, (b) 650, (c) 750, and (d) 810 °C.

IV. DISCUSSION

A. Effects of RTA on the Ce^{3+} environment

Two proposed mechanisms leading to a decrease in linewidth of the nearly cubic Ce^{3+} resonance with anneal temperature are (i) a breakup of Ce^{3+} clusters or (ii) a more uniform Ce^{3+} crystal field. It is unlikely that Ce^{3+}–Ce^{3+} clusters will occur during sputtering deposition since migration of ions during low-temperature film growth is difficult. This is especially true since the Ce ions are electrostatically repelled from each other. Figure 7 show the FWHM of the XRD diffraction peaks and the linewidth of the nearly cubic Ce^{3+} center for the SrS:Ce,Ga films annealed at various temperatures. Qualitatively similar trends are observed for the SrS:Ce thin films (not shown). The FWHM of the XRD peaks and the EPR spectra show that the linewidth of the nearly cubic Ce^{3+} resonance markedly decreases as the anneal temperature increases. These observations appear best described by the postulation that crystal field around the Ce^{3+} ion becomes more uniform with increasing anneal temperature. It appears that the improved crystallinity is the impetus behind the more local uniform crystal field. The linewidth of the $Ce^{3+}-V_{Sr}$ sites may also change with RTA but

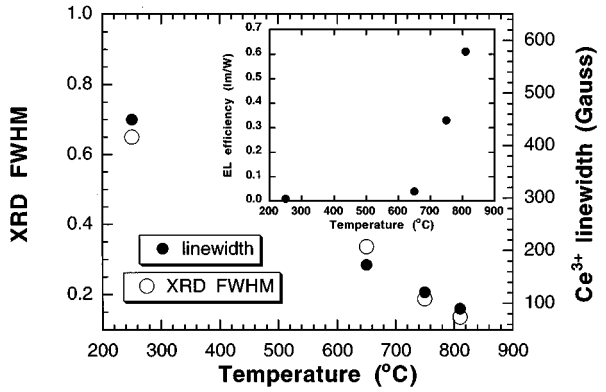

FIG. 7. Plot of the FWHM of the XRD diffraction peaks and the linewidth of the nearly cubic Ce^{3+} EPR resonance in SrS:Ce,Ga thin films for the various RTA temperatures studied. The inset shows the effect of the RTA on EL efficiency.

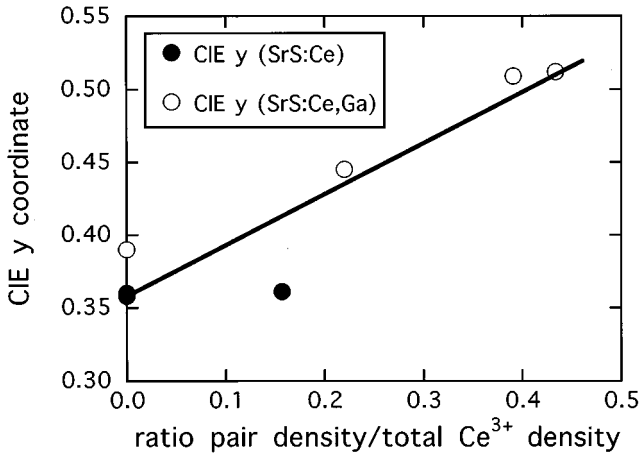

FIG. 8. CIE y coordinate plotted as a function of the ratio of the $Ce^{3+}-V_{Sr}$ site density to the total Ce^{3+} site density.

this is very difficult to monitor given that the signal is quite weak, and we can only observe the perpendicular transition.

B. Correlations between EPR and EL responses

1. Total Ce^{3+} density, crystal field uniformity, and EL performance

We now relate the EPR response to the EL of the SrS:Ce and SrS:Ce,Ga devices. Table II for the SrS:Ce films shows that the EL efficiency increases as the total Ce^{3+} density increases at higher annealing temperatures. For the SrS:Ce,Ga films (Table II), however, there are large increases in efficiency when the RTA temperature is increased from 650 to 810 °C, but the Ce^{3+} density remains relatively constant. These results show that the *total* density of Ce^{3+} ions in the SrS lattice is not the only factor that affects EL efficiency. We consistently observe that as the uniformity in the near cubic Ce^{3+} environment improves (along with film crystallinity), so does the EL performance, as illustrated in the inset of Fig. 7 for the SrS:Ce,Ga films.

2. Defects and EL performance

We expect that the improved EL efficiency with increased RTA temperature also involves a disappearance and/or reconfiguration of intrinsic and/or extrinsic defects. These defects, created by the nonequilibrium film growth associated with the sputtering process, can act as nonradiative pathways or traps to reduce luminescent efficiency.[5,6] Intrinsic defects include *isolated* S and Sr vacancies. As an example of defect reconfiguration that may enhance EL performance, the data already presented suggest that it is possible that isolated V_{Sr} vacancies can migrate to Ce sites to form $Ce^{3+}-V_{Sr}$ complexes during annealing.

3. Ga versus non-Ga doped SrS:Ce films

We now examine differences between the SrS:Ce and SrS:Ce,Ga EL devices. We concentrate on the differences between the two types of films after annealing at $T \geqslant 750$ °C. As Tables I and II show, EL efficiency rises markedly with annealing temperature. Two parameters that also increase at these higher temperatures are the density of $Ce^{3+}-V_{Sr}$ pair centers and the crystalline perfection (as measured by the narrowness of the nearly cubic Ce^{3+} linewidth, or the FWHM of the XRD peaks). Of these two parameters, the correlation of EL efficiency and brightness with the latter appears to be the most consistent. However, it is also possible that the presence of $Ce^{3+}-V_{Sr}$ pairs is a significant driving force for improved EL as discussed earlier. More work is clearly needed to establish this causality, however.

The SrS:Ce,Ga samples exhibit a greenshift in the emitted light when compared to the SrS:Ce films (Figs. 1 and 2 and Tables I and II). This greenshift in the emitted light might be expected if the concentration of Ce increases,[9,20] promoting Ce^{3+}–Ce^{3+} interactions, or if the crystal field symmetry is lowered; a lower symmetry crystal field will lower the energy of the lowest excited state ($5d$) component from which the emission originates.[21,22] However, changes in the Ce^{3+} density are not always accompanied by changes in the CIE coordinates (Table I), thus the Ce^{3+} density, alone, is not a good predictor of the greenshift.

To understand the origin of the greenshift, it is instructive to compare the EL and EPR of the SrS:Ce devices annealed at 810 °C to the SrS:Ce,Ga devices annealed at 750 °C. The linewidth and density of the nearly cubic Ce^{3+} resonance are essentially the same in these two samples as in the grain size (110 vs 120 nm) and FWHM of the XRD peaks. However, the CIE coordinates of the SrS:Ce,Ga film are quite different than that of the SrS:Ce film. In fact, the one major difference between these two samples is the density of $Ce^{3+}-V_{Sr}$ sites ($<0.3\times10^{19}/cm^3$ vs $1.0\times10^{19}/cm^3$). If the $Ce^{3+}-V_{Sr}$ site is indeed luminescent, it could lead to the greenshift in the emitted color since it is a *lower-symmetry* site than the isolated nearly cubic Ce^{3+} site. In support of this conjecture, Fig. 8 shows that the CIE y coordinate increases as the ratio of $Ce^{3+}-V_{Sr}$ sites to the total Ce^{3+} site density increases for both the SrS:Ce and SrS:Ce,Ga thin film devices. Molecular orbital calculations[23] of the effect of such a vacancy on the Ce^{3+} transitions are consistent with a greenshift of the spectrum.

We now discuss the possibility that the greenshift can be caused by reabsorption of the blue Ce^{3+} emission. For the films studied here, the Ce concentration is very low, approximately 0.06 at. %. At this Ce concentration level, Huttl *et al.*[5] estimate that the absorption coefficient at 440 nm for Ce^{3+} is 10^2/cm. Thus, for the film thicknesses used in this study (10^{-4} cm), less than 1% of the light will be reabsorbed. Less than 1% reabsorption of the emitted light will not cause the rather large greenshifts observed in this study for the SrS:Ce,Ga films.

Last, it has been proposed in the literature[5,22,24,25] that charge compensation of Ce^{3+} ions in SrS:Ce materials can occur via self-compensation due to V_{Sr}. We observe that besides isolated singly positively charged Ce^{3+} sites there are Ce^{3+} sites intimately associated with doubly negatively charged V_{Sr}, for a total charge of -1. Generally speaking, it is not possible to account for charge compensation via EPR since the isolated V_{Sr} are not paramagnetic and cannot be quantitatively measured. Thus, it is perhaps fortuitous that charge neutrality can be accounted for via the EPR measurements in the SrS:Ce,Ga samples annealed at 810 °C. In those samples approximately half of the nearly cubic Ce^{3+} sites are isolated (not associated with a nearby V_{Sr} vacancy and, thus, singly positively charged), while the other half are associated with a doubly negatively charged V_{Sr}, giving these sites a net charge of -1 (Table II).

V. CONCLUSIONS

In summary, we suggest that the emitted light spectrum and EL efficiency of SrS:Ce films depend on the local environment at the Ce^{3+} ion. TEM and XRD results show that rapid thermal annealing of the SrS:Ce films improves film crystallinity which concurrently leads to a more uniform crystal field environment around the cubic Ce^{3+} site. The improved crystal field appears to be involved in the improvement of EL efficiency of the devices. The annealing of SrS:Ce,Ga films also results in the formation of another type of Ce^{3+} site believed to be associated with nearby V_{Sr}. It is proposed that these centers can cause a greenshift in the emitted color and may lead to more efficient light emission.

ACKNOWLEDGMENTS

The part of this work performed at Sandia National Laboratories was supported by DARPA and the U. S. Department of Energy under Contract No. DE-AC04-94AL85000. Sandia is a multiprogram laboratory operated by Sandia Corporation, a Lockheed Martin Company, for the U. S. Department of Energy. The work at the University of Florida was supported by DARPA Grant No. MDA972-93-1-0030 through the Phosphor Technology of Excellence.

[1] C. N. King, J. Soc. Inform. Display **4**, 153 (1996).
[2] H. Kobayashi and S. Tanaka, J. Soc. Inform. Display **4**, 157 (1996).
[3] L. Ozawa, *Cathodoluminescence* (VCH, New York, 1990).
[4] W. A. Barrow, R. E. Coovert, and C. N. King, SID '84 Int. Symp. Dig. 249 (1984).
[5] B. Huttl, U. Troppenz, K. O. Velthaus, C. R. Ronda, and R. H. Mauch, J. Appl. Phys. **78**, 7282 (1995).
[6] S.-S. Sun, T. Nguyen, M. S. Bowen, J. Kane, P. N. Yocum, A. Naman, K. Jones, P. H. Holloway, D. R. Evans, and W. M. Dennis, Phosphor Technology Center of Excellence extended abstract, 1996.
[7] H. Ohnishi, SID '94 Int. Symp. Dig. 129 (1994).
[8] E. Soininen, M. Leppanen, and A. Pakkala, Proceedings of the 13th International Display Research Conference, Strasbourg, France, 1993, p. 233.
[9] C. Fouassier and A. Garcia, *Inorganic and Organic Electroluminescence/EL 96 Berlin,* edited by R. H. Mauch and E.-E. Gumlich (Wissenschaft und Technik, Berlin, 1996), p. 313.
[10] B. Huttl, U. Troppenz, H. Venghaus, R. H. Mauch, J. Kreissl, A. Garcia, C. Fouassier, P. Benalloul, C. Barthou, J. Benoit, F. Gendron, and C. Ronda, Mater. Sci. Forum **182-184**, 263 (1995).
[11] W. L. Warren, K. Vanheusden, C. H. Seager, D. R. Tallant, J. A. Tuchman, S. D. Silliman, and D. T. Brower, J. Appl. Phys. **80**, 7036 (1996).
[12] P. C. Taylor and P. J. Bray, J. Magn. Reson. **2**, 305 (1970).
[13] J. Kreissl, B. Huttl, U. Troppenz, K. X. Vlthaus, R. H. Mauch, and C. Fouassier, in Ref. 9, p. 177.
[14] A. Abragram and B. Bleaney, *EPR in Transition Metal Ions* (Dover, New York, 1970).
[15] W. L. Warren, K. Vanheusden, D. R. Tallant, C. H. Seager, S.-S. Sun, D. R. Evans, W. M. Dennis, E. Soininen, and J. A. Bullington, J. Appl. Phys. **82**, 1812 (1997).
[16] D. T. Petasis, G. H. Bellesis, N. S. Vander Ven, and S. A. Fridberg, J. Appl. Phys. **70**, 5998 (1991).
[17] J. Kreissl, Phys. Status Solidi B **180**, 441 (1993).
[18] J. E. Wertz and J. R. Bolton, *Electron Spin Resonance* (Chapman and Hall, New York, 1986), p. 157.
[19] The isolated near cubic $Ce^{3+}(V_{Sr})$ site is singly positively charged (doubly negatively charged) with respect to the neutral lattice. Thus, the $Ce^{3+}-V_{Sr}$ center can be described as a defect dipole. Defect dipoles consisting of vacancies associated with substitutional dopants for charge compensation are quite common in many material systems [E. Siegel and K. A. Muller, Phys. Rev. B **19**, 109 (1979)].
[20] A. Kato, M. Katayama, K. Sugiura, K. Inoguchi, H. Ishihara, N. Ito, and T. Hattori, Bull. Res. Inst. Electron. **30**, 199 (1995).
[21] G. Blasse and B. C. Grabmaier, *Luminescent Materials* (Springer, Berlin, 1994), p. 46.
[22] B. Huttl, K.-O. Velthaus, U. Troppenz, J. Kreissl, and R. H. Mauch, in Ref. 9, p. 319.
[23] T. O'Brian, P. D. Rack, M. Zernerad, and P. H. Holloway (unpublished).
[24] W. Lehmann, J. Lumin. **5**, 87 (1972).
[25] P. K. Ghosh and B. Ray, Prog. Cryst. Growth Charact. Mater. **25**, 1 (1992).